Geophysical Research Letters

RESEARCH LETTER
10.1029/2019GL082077

Special Section:
The Three Major Hurricanes of 2017: Harvey, Irma and Maria

Key Points:
- Hurricane Maria was the most extreme rainfall event when compared to 129 tropical cyclones
- Return periods for Hurricane Maria's precipitation decreased by at least half across Puerto Rico, indicating increased likelihood in recent years
- The probability of Maria's heaviest precipitation has likely increased as a result of long-term climate trends

Supporting Information:
- Supporting Information S1
- Figure S1

Correspondence to:
D. Keellings,
djkeellings@ua.edu

Citation:
Keellings, D., & Hernández Ayala, J. J. (2019). Extreme rainfall associated with Hurricane Maria over Puerto Rico and its connections to climate variability and change. *Geophysical Research Letters*, *46*, 2964–2973. https://doi.org/10.1029/2019GL082077

Received 17 JAN 2019
Accepted 25 FEB 2019
Accepted article online 4 MAR 2019
Published online 12 MAR 2019

Extreme Rainfall Associated With Hurricane Maria Over Puerto Rico and Its Connections to Climate Variability and Change

David Keellings[1] and José J. Hernández Ayala[2]

[1]Department of Geography, University of Alabama, Tuscaloosa, AL, USA, [2]Department of Geography, Environment, and Planning, Sonoma State University, Rohnert Park, CA, USA

Abstract Hurricane Maria was associated with record-breaking rainfall over Puerto Rico and caused unprecedented flooding and landslides. Here we analyze the extreme rainfall produced by Hurricane Maria using 35 stations with daily precipitation data from 1956–2016. A covariate-based extreme value analysis point process approach that accounts for natural climate variability and long-term climate change influences on extreme rainfall is applied. Hurricane Maria produced the single largest maximum rainfall event since 1956 and had the highest total averaged precipitation of 129 storms that have impacted the island since 1956. Return periods for an event of Hurricane Maria's precipitation magnitude decreased in 48.6% of stations across Puerto Rico and at least halved when averaged across the island. Within the most affected areas it is likely that the probability of precipitation of Maria's magnitude has increased by a factor greater than 1 (best estimate 4.85) as a result of long-term climate trends.

Plain Language Summary Hurricane Maria was associated with record-breaking rainfall over Puerto Rico, which caused unprecedented flooding and landslides across the island and led to widespread devastation. Here we analyze the extreme rainfall produced by Hurricane Maria using 35 historical weather stations with daily precipitation data from 1956–2016. We use a statistical analysis technique to determine how unusual Maria's rainfall was and if Maria's rainfall can be attributed to climate variability and/or climate change. We find that Hurricane Maria produced the single largest maximum rainfall event since 1956 and had the highest precipitation of 129 storms that have impacted the island since 1956. Our study concludes that extreme precipitation, like that of Hurricane Maria, has become much more likely in recent years and long-term trends in atmospheric and sea surface temperature are both linked to increased precipitation in Puerto Rico. These results place Maria prominently in the context of extreme storms that have impacted Puerto Rico and indicate that such events are becoming increasingly likely.

1. Introduction

On 20 September 2017, Hurricane Maria made landfall on the southeast coast of Puerto Rico as a strong Category 4 hurricane. Tropical cyclones (TCs) are not uncommon to the island, the long-term average for TC landfalls in the northern Caribbean where Puerto Rico is located is one per year (Pielke et al., 2003), the National Hurricane Center Report (2018) on Maria highlights it as the strongest hurricane to make landfall on the island since 1928 (Pasch et al., 2018). Maria broke rainfall records that resulted in unprecedented flooding and mudslides and combined with sustained winds of 249 km/hr at landfall that contributed to a near complete loss of the electrical grid and municipal water supplies for 3.4 million residents (Pasch et al., 2018). All infrastructure was affected with 80% destruction of communication systems, including utility poles and cellular towers, and ultimately the storm resulted in a cost of 90 billion dollars in damage between Puerto Rico and the U.S. Virgin Islands, which exceeds the previously most costly storm to affect Puerto Rico directly, Hurricane Georges in 1998, by 85 billion dollars (Pasch et al., 2018). The official death toll of Hurricane Maria is 64 deaths, though a mortality study by Kishore et al. (2018) found the number of excess deaths associated with Maria is more than 70 times the official estimate bringing the total count closer to 5,000. Disaster-related deaths are difficult to determine. While direct causes of death, such as flying debris or drowning, are relatively easy to assign, indirect deaths resulting from delayed medical treatment or worsening of preexisting conditions are much more difficult to capture (Kishore et al., 2018). Further hindering this effort in Puerto Rico is the requirement that every hurricane-related death be confirmed by the Institute of Forensic Sciences, which requires bodies to be brought to San Juan and delays the issuance of a death certificate (Kishore et al., 2018). A recent report concluded that the total excess mortality associated with Hurricane Maria in Puerto Rico was 2,975, which is 46 times the official government estimate (Santos-Burgoa et al., 2018). Additionally, estimates of between 114,000 and 212,000 residents are expected to migrate away from the island in the first year, and up to 14% of the total population by the end of the second year following the event (Meléndez & Hinojosa, 2017).

Several recent studies have focused on the relationship between climate change and the intensity of hurricanes. Mann and Emanuel (2006) found that the underlying factors in the increasing trends of Atlantic hurricane intensity appear to be the influence of primarily anthropogenic forced large-scale warming, while Elsner (2006) found causal evidence that increasing near-surface air temperatures lead to an increase in sea surface temperature (SST) as evidence to support a hypothesis of human-induced climate change influencing the intensity of TCs in the Atlantic. No trend in hurricane frequency has been detected. Other studies have looked at the influences that teleconnections, such as the El Nino–Southern Oscillation (ENSO), and anthropogenic influences, such as carbon dioxide (CO_2), have on hurricane rainfall variability. A recent study by Risser and Wehner (2017) used a covariate-based extreme value analysis (EVA) approach where they found that human-induced climate change likely increased Hurricane Harvey's total rainfall by at least 19% and increased the chance of the observed precipitation by a factor of at least 3.5. Emanuel (2017) examined the annual probability of Hurricane Harvey's observed rainfall finding that it had become 6 times more likely since the end of the twentieth century and that a similar magnitude event will be roughly 18 times more likely by 2081–2100. Another study found that Hurricane Harvey was 3 times more likely due to anthropogenic climate change (Van Oldenborgh et al., 2017). Patricola and Wehner (2018) examined the anthropogenic influence on major TCs finding that relative to preindustrial conditions, climate change has intensified extreme rainfall in Hurricanes Katrina, Irma, and Maria.

Here we focus on two main questions regarding the rainfall associated with Hurricane Maria. How does the extreme rainfall associated with Hurricane Maria compare to the precipitation climatology of TCs in Puerto Rico and how much of the rain attributed to the storm can be explained by natural climate variability and anthropogenic climate change? To address these questions, data from 47 sites are used to estimate Hurricane Maria's rainfall over the 3-day period the storm was within a 500-km radius of the island. Historical data from 35 stations are used in an EVA point process model to examine the relationship between modes of natural variability (North Atlantic Oscillation [NAO], Atlantic Multidecadal Oscillation [AMO], and ENSO), long-term trends associated with anthropogenic climate change (atmospheric CO_2, global temperature, SST, and Cloud cover), and the extreme rainfall associated with Hurricane Maria. Changes in return periods associated with Maria's peak precipitation are estimated for each of 35 historical stations.

2. Data

Six-hourly TC positions were extracted from the International Best Track Archive for Climate Stewardship for the years 1970–2017 (Knapp et al., 2010). A Geographic Information System was utilized to calculate a 500-km buffer around the island, allowing us to define the portion of Maria's track that was within the radius. Maria spent 3 days within the radius from 19 to 21 September 2017. This method has been used by researchers examining TC rainfall in Puerto Rico and the extreme floods associated with those events (Hernández Ayala et al., 2017; Hernández Ayala & Matyas, 2016, 2018). Those studies identified 86 TCs within the 500-km radius around Puerto Rico from 1970–2010. In this study we expanded their data set to include an extra 43 TCs that were within the 500-km radius during 1956–1970 and 2011–2017 for a total of 129 storms.

Daily rainfall totals were obtained from the National Centers for Environmental Information (NCEI) for 19 stations and from the U.S. Geological Survey for 28 rain gauges with daily data for Hurricane Maria, for a total of 47 sites. Daily rainfall totals were obtained from the NCEI for 35 historical stations with a minimum of 70% of observations during the hurricane season that spans from 1 June to 30 November for a period that begins 1 June 1956 and ends 30 November 2016. A recent study examining extreme rainfall associated with Hurricane Harvey in Texas used a similar data coverage percentage to examine the storm's relationship with climate variability and change (Risser & Wehner, 2017).

The teleconnection indices were obtained from the Climate Prediction Center. The Niño 3.4 SST standardized anomalies are part of the ERSSTv5 monthly index from the National Oceanic and Atmospheric

Administration's National Center for Environmental Prediction (http://www.cpc.ncep.noaa.gov/data/indices/). We used the NAO index constructed by projecting the daily (00Z) 500-mb height anomalies over the Northern Hemisphere onto the leading mode of variability in the NAO (Hurrell, 1995). The AMO index used is based on North Atlantic SST anomalies calculated from detrended long run averages of mean SST observations (Enfield et al., 2001). Global mean CO_2 measurements are a combination of data obtained from the International Institute for Applied Systems Analysis or IIASA (see https://tntcat.iiasa.ac.at/RcpDb) available for 1950–2005 and the record from the Mauna Lua Observatory available for 1958–2017.

Global mean surface temperature data were obtained from the National Aeronautics and Space Administration Goddard Institute for Space Science surface temperature analysis (Hansen et al., 2010). Monthly mean SST data (extended reconstructed SST V5) for a section of the Atlantic Ocean where TCs that impact Puerto Rico develop (12 N, 30 N and 45 W, 80 W) were obtained from the National Oceanic and Atmospheric Administration's Earth Systems Research Lab for 1956–2017. Monthly mean cloud cover data for the same section of the Atlantic Ocean were obtained from the International Comprehensive Ocean-Atmosphere Data Set for 1956–2017. It is well known that there is a relationship between warm Atlantic SSTs and the intensity and frequency of major TCs (Emanuel, 2005, Webster et al., 2005), and for that reason SSTs in a section of the Atlantic, where a significant increasing trend in SSTs has been found (Deser et al., 2010), were examined in this study. Since cloud cover is highly influenced by changes in SST, it was also included as one of the independent variables in this study.

3. Methods

3.1. Spatial Interpolation

The mean total average and the maximum rainfall were extracted from the 3-day precipitation totals for Hurricane Maria for the dates (19–21 September) that the storm was within a 500-km radius of Puerto Rico. The mean total average and maximum rainfall for Hurricane Maria were then compared to the other 129 TCs that have impacted Puerto Rico since 1956. Geostatistical interpolation was combined with historical observations in order to maximize the available record for analysis as only 7 of the 35 historical stations remained operational during the passage of Maria. An inverse distance weighted and ordinary kriging (OK) surface of maximum rainfall for Hurricane Maria were constructed from the 47 stations with data for the 3-day period in order to examine the spatial distribution of extreme precipitation associated with the event. The inverse distance weighted and OK surfaces were highly correlated (0.930), and the OK interpolated surface was then used to extract the maximum rainfall for each of the 35 historical station locations. The OK method has been used previously in Puerto Rico to examine the spatial distribution of TC rainfall and its relation to extreme floods (Hernández Ayala et al., 2017; Hernández Ayala & Matyas, 2018).

We have divided the stations on the island into two regions. The entire island forms the large region containing all 35 stations. The small region contains 19 stations. Stations were grouped in this way to differentiate between Hurricane Maria's precipitation impact on the entire island as a whole versus the diagonal swath of Maria from southeast to northwest where the highest precipitation values (>300 mm) were recorded (Figures 1a and 1b). Puerto Rico historically exhibits high spatial variability in hydrology given its varied topography and diverse precipitation formation mechanisms (Hernández Ayala et al., 2017). This variability is illustrated in Maria's rainfall with some stations at low elevation in the east and west periphery of the island experiencing much lower precipitation than those closer to Maria's track or those at higher elevation.

3.2. EVA

An EVA was conducted for each of the 35 historical stations individually based on daily precipitation time series for the hurricane seasons of 1956–2016. The 2017 observations were intentionally excluded to provide an out-of-sample analysis of Hurricane Maria. We use a point process approach to EVA and extend it to incorporate atmospheric variables (Coles, 2001). Such an approach has previously been used to examine the influence of covariates on extreme meteorological values (Furrer et al., 2010; Keellings & Waylen, 2014; Photiadou et al., 2014) and more recently, in block maxima form, to attribute risk of individual events (Risser & Wehner, 2017). The point process approach is advantageous in that far more of the information about the upper tail of the distribution is available than would be possible using a smaller sample of block maxima (Coles, 2001). A relative threshold equivalent to the 99th percentile of observations at each station

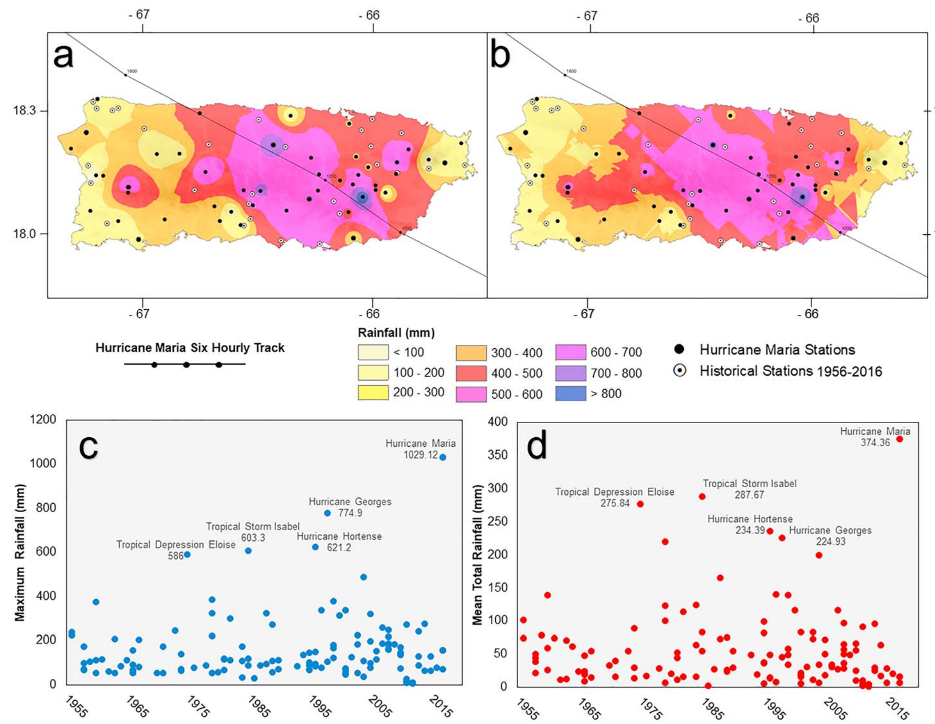

Figure 1. Maximum daily rainfall interpolated surfaces for Hurricane Maria using inverse distance weighted (a) and ordinary kriging (b). Island maximum (c) and island mean total rainfall (d) from 129 historical tropical cyclones with the top five storms labeled.

is used to define an extreme data series of precipitation events crossing this threshold. These extreme events are said to be part of a Poisson process as they are occurring randomly and at a variable rate (Coles, 2001). Statistical theory states that maximizing the likelihood of this Poisson process leads to estimates of the parameters μ (location or central tendency), σ (scale or variance), and ξ (shape or skew) of the limiting generalized extreme value (GEV) distribution of the corresponding block maximum (Coles, 2001). The cumulative distribution function of the GEV is given by

$$P(x) = \exp\left[-\left\{1+\xi\frac{x-\mu}{\sigma}\right\}^{\frac{-1}{\xi}}\right]$$

Multiple covariates are introduced into the estimation of GEV parameters such that those parameters are allowed to vary over time and thus characterize changes in the distribution of extreme precipitation events over time. Multiple covariates are used: annually averaged Niño3.4 index, annually averaged AMO index, seasonally averaged NAO index, seasonally averaged global CO_2, global mean surface temperature, seasonally averaged SST, and cloud cover. These covariates were chosen as they are known to influence TC activity in the Atlantic, and they provide a clear distinction between modes of natural variability and long-term change associated with human influences (Hernández Ayala & Matyas, 2016; Patricola et al., 2014; Risser & Wehner, 2017).

The covariates are introduced as non-stationary signals in Generalized Linear Models of both the location and log-transformed scale parameters of the GEV such that

$$\mu(x) - \beta_{0_{(i)}} + \beta_{1(i)}x$$
$$\ln\{\sigma(x)\} = \beta_{0_{(i)}} + \beta_{1(i)}x$$
$$\xi(x) = \beta_{0(i)}$$

where $\beta_{0(i)}$ are the stationary model parameter estimates and $\beta_{1(i)}x$ are linear transformations of the time-varying covariates (Coles, 2001). The shape parameter, ξ, was modeled as an intercept only term as this parameter is numerically difficult to estimate with any accuracy (Katz et al., 2002). All possible linear combinations of covariates are examined and Akaike information criterion (AIC) in combination with the likelihood ratio test is used to select the best model, as this is most appropriate for comparing nested models fitted with fixed maximum likelihood estimation (Coles, 2001). The best estimates of all statistical parameters in the AIC/likelihood ratio test selected model are obtained through maximum likelihood estimation (MLE), and bootstrapping is used to quantify uncertainty in these estimates (see the supporting information for more details). From these estimates return values (corresponding to the quantiles of the distribution of extreme precipitation), return probabilities (the probability of a particular magnitude of precipitation), and return periods (the inverse return probability) are calculated.

4. Results

As a tropical island, Puerto Rico receives a lot of precipitation, especially in the north and central regions of the island, where rainfall can range from 3,000–4,300 mm annually (Colon & Jose, 2009). Out of 129 storms that impacted Puerto Rico since 1956, including those to hit directly or within a 500-km radius of the island, the extreme rainfall associated with Hurricane Maria had the largest maximum daily precipitation of 1,029 mm, equivalent to over one fourth of the average total annual rainfall at the wettest location on the island at the Yunque National Rainforest. Overall, Hurricane Maria exhibited the highest values in maximum daily precipitation (based on all days when storm was within 500 km of island) and total mean precipitation (mean precipitation total from that accumulated at each station while storm within 500 km of island) when compared to the other 128 TCs that have impacted Puerto Rico since 1956 (Figures 1c and 1d). Hurricane Maria exhibited a 30% increase from the previous TC-related highest total mean rainfall event (Tropical Storm Isabel in 1985; José J. Hernández Ayala & Matyas, 2018). When compared to Hurricane Georges, the last major storm to make landfall on the island in 1998, and previously the costliest weather event, Maria exhibited a 66% increase in island mean total rainfall and a 33% increase in island maximum total precipitation.

Previous work of Hernández Ayala and Matyas (2016) found that extreme rainfall (>50 mm) occurred across Puerto Rico when a storm center passed within a distance of 233 km or less, total precipitable water (TPW) exceeded 44.5 mm, midlevel relative humidity was greater than 44.5%, and horizontal translational speed measured at 6.4 m/s or less. Hurricane Maria exceeded those thresholds with a TPW of 51.5 mm, a midlevel relative humidity of 53%, and an average horizontal translational speed of 3.65 m/s between 19 and 21 September, considering measurements before and after landfall on the island. In perspective of past events, Tropical Storm Eloise (1975) and Hurricanes David (1979), Hortense (1996), and Georges (1998) triggered flash floods and mudslides that caused combined losses of more than 3 billion dollars and more than 50 fatalities over the island (Bennett & Mojica, 1998; Hebert, 1976, 1980; J.J. Hernández Ayala et al., 2017; Pasch et al., 2001; Pasch & Avila, 1999) yet all of these impacts combined do not match the life and economic losses associated with Hurricane Maria.

Hurricane Maria's highest precipitation peaks were clustered in the eastern region of the island, especially in the southeast where a station recorded 1,029 mm of rain on 20 September 2017 (Figure 1). Hurricane Maria's precipitation decreased from east to west, with the exception of an area in the interior west where some sites recorded values between 300 and 500 mm. The spatial pattern of maximum rainfall associated with Hurricane Maria (higher east and lower west) is generally similar to that exhibited when TCs approach within 220 km of Puerto Rico's coast and are embedded in moisture environments of 50 mm of TPW (José J. Hernández Ayala & Matyas, 2018).

Return period estimates for Maria's observed maximum daily precipitation are shown in Figure 2a. Results from the EVA show 10% to almost 100% reductions in Maria's estimated return period through the record across much of the island (Figure 2b) and a significant (as per Mann-Kendall test; Kendall, 1955) decreasing trend in return period estimates of Maria's maximum daily precipitation at 17 of the 35 stations, which suggests that a rainfall event of the magnitude of Hurricane Maria has become more likely at these locations (Figure 2c). The changes in return periods were estimated from GEV parameters of stationary or null models fitted to moving windows of 30 years through the record 1956–2016, at stations where inclusion of covariates offered no model improvement, and by allowing GEV parameters to vary through time with covariates, at stations where inclusion of covariates improved model fit. The majority of stations show a decreasing

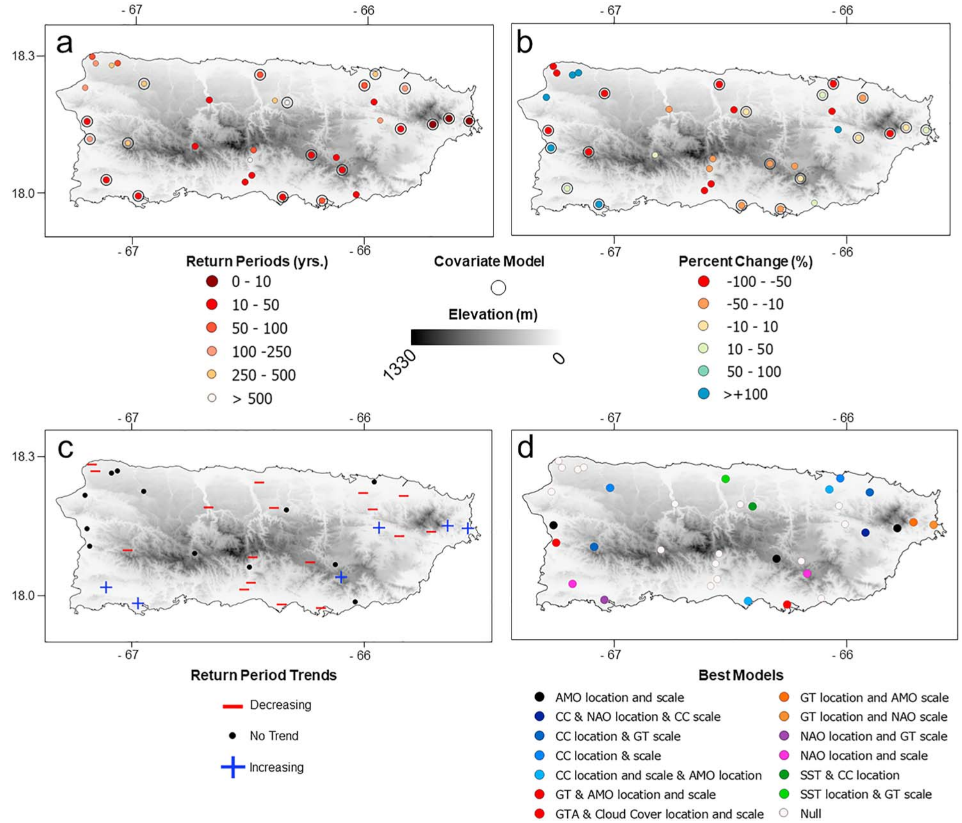

Figure 2. (a) Estimates of Maria's maximum daily precipitation return period at 35 historical stations (using the ordinary kriging interpolation estimates). (b) Percent change in estimate of Maria's maximum daily precipitation return period between beginning and end of record (1956–2016). A circular outline is shown to highlight stations where a covariate model was selected over the null model. (c) Stations with positive, no trend, or negative trends in estimated return periods. (d) Extreme value analysis point process selected best models at each of the 35 stations with covariate and related generalized extreme value parameter indicated. AMO = Atlantic Multidecadal Oscillation; NAO = North Atlantic Oscillation; SST = sea surface temperature; CC = cloud cover; GT = global mean surface temperature; GTA = global surface temperature anomalies.

trend in return period (Figure 2c). Six stations exhibit increasing trends in return periods that may be explained by the highly variable nature of TC rainfall in the central and western regions of the island and influence of varied precipitation mechanisms (Colon & Jose, 2009; José J. Hernández Ayala & Matyas, 2018).

When return period estimates of Maria's maximum daily precipitation are averaged within the large and small regions, we find that estimated return periods and their 90% confidence intervals are decreasing through the record in both regions (Figures 3a and 3b). The return period estimate has decreased from approximately 300 to 115 years corresponding to a roughly threefold increase in return probability in the large region. In the small region, the return period estimate has decreased from approximately 290 to 152 years corresponding to a roughly twofold increase in return probability.

The AIC and likelihood ratio test selected best models include covariates at 19 stations (54.3%) indicating statistically significant relationships between extreme rainfall and the climate variability and change variables, predominantly AMO, NAO, global temperature, and cloud cover (Figure 2d). Eleven of these stations are located within the small region. These results suggest that fluctuations in SSTs in the Atlantic (as indicated by the AMO and NAO indices) in combination with the long-term upward trend in global temperatures and cloud cover are related to extreme rainfall events in Puerto Rico. It is also of note that ENSO offered no model improvement and was thus not included as a covariate in any model.

The covariate-based EVA models permit exploration of the effects of those covariates on extreme precipitation so that we may isolate the effects of modes of natural and long-term anthropogenic sources of variation.

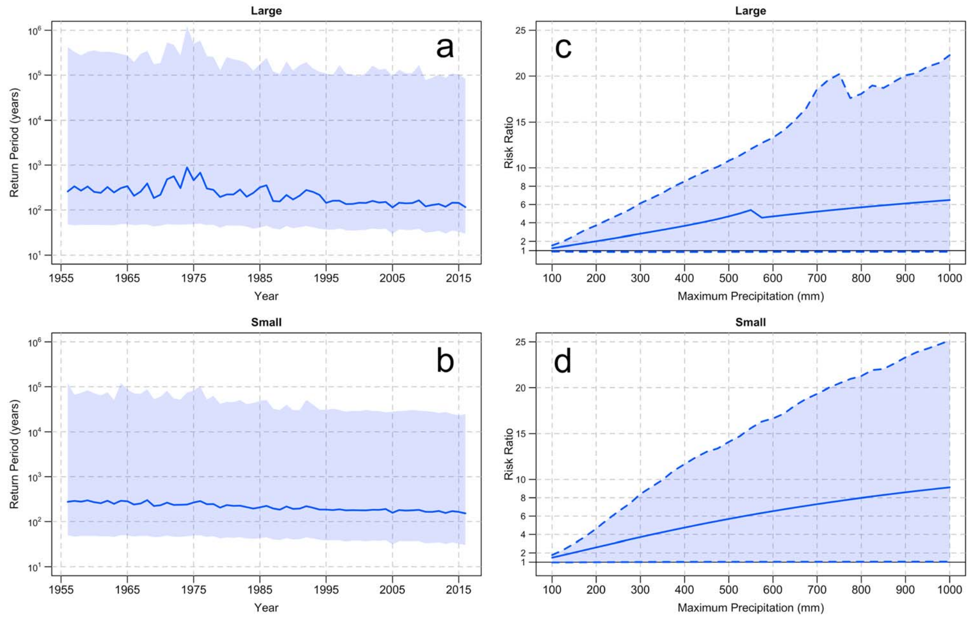

Figure 3. Return period for observed Hurricane Maria maximum daily precipitation with 90% confidence interval using the kriged station average for the large (a) and small (b) regions. Risk ratio comparing the probability of a range of peak storm precipitation for 2017 values of all covariates versus 1956 values of long-term trend covariates holding all other covariates constant at observed 2017 values (solid line) for the large (c) and small (d) regions. Likely (66%) confidence bound shown as dashed line.

This is possible through comparison of conditional probabilities of event magnitude in actual versus counterfactual realities. First, the covariate model can be used to estimate the probability of exceeding, Z, above some threshold, z, of precipitation conditional upon observed 2017 values of the covariates, for example, AMO and global temperature:

$$p_1(z) \equiv P(Z > z | 2017 \text{ values of AMO and global temperature})$$

Second, the probability of Z exceeding threshold z is calculated again, but in the counterfactual reality of 2017 observed AMO and 1956 observed global temperature:

$$p_0(z) \equiv P(Z > z | 2017 \text{ value of AMO, 1956 value of global temperature})$$

The likelihood of these two events can then be compared using the risk ratio as is commonly used in probabilistic event attribution (National Academies of Sciences, Engineering, and Medicine, 2016; Pall et al., 2014; Risser & Wehner, 2017):

$$RR(z) = \frac{p_1(z)}{p_0(z)}$$

Here risk refers to the relative risk of the event under observed conditions versus the counterfactual reality. Figures 3c and 3d show the best estimates of this risk ratio for a range of storm event peak precipitation (100–1,000 mm) for the large and small regions. Only stations where the best model included long-term trend covariates (atmospheric CO_2, global mean surface temperature, SST, and cloud cover) were included in calculation of risk ratios. The small region comprised 9 (of 17 stations, 53%) stations with long-term covariates identified in the best model and the large region comprised 14 (of 35 stations, 40%) stations. The best estimates of risk ratios in both regions are above one for the entire range of maximum daily precipitation. However, the likely lower bound is below one in the large region and thus not statistically significant. For Maria's mean maximum daily precipitation (large region: 350 mm, small region: 412 mm) the best estimates of the risk ratio are 3.22 (lower bound 0.79) for the large region and 4.85 (lower bound 1.02) for the small region. These lower bound estimates are notably static across the range of maximum precipitation and thus insensitive to observational uncertainty. The step change at around 550 mm in Figure 3c is caused by a single station, in the large region, exhibiting a negative shape parameter value in the fitted GEV model. A negative shape parameter indicates a thin upper tail of precipitation and a bounded distribution that reaches an upper limit. In reality statistical precipitation distributions are bounded, but it is not uncommon to fit unbounded distributions as is the case for all other stations on the island (Cooley et al., 2007; Risser & Wehner, 2017). Concordant patterns of estimated return periods and risk ratios were found under identical analysis using only data from the seven stations that remained operational during the passage of Maria (see the supporting information).

As with other attribution studies using similar statistical methods applied to observational data, as was done here, it is essential to be aware that these results should only be interpreted in the Granger causality sense (Granger, 1969). As such, these results cannot prove any causal relationships, but they can make risk ratio attribution statements to climate trends. For Hurricane Maria's precipitation over Puerto Rico our models suggest that there is a likely increase in the chance of observing Maria's peak precipitation, which is attributable to long-term climate trends, at over half of the stations in the small region as the likely lower bound risk ratio is above one. In the large region, less than half of the stations exhibit an increase in the risk ratio and the likely lower bound is below one.

5. Conclusions

In the sense of the historical record, Hurricane Maria was an unprecedented storm event for Puerto Rico. The island has not been impacted by a storm producing as much peak or total precipitation at any time during the past 60 years. In a statistical sense, Maria's precipitation is an extreme outlier in the historical record at most locations across the island and as such may have been the result of physical processes that were not present during 1956–2016. As EVA provides an estimated limiting GEV distribution based on observations, it is, therefore, limited by those observations in providing a statistical representation of underlying physical processes. In this study, the out-of-sample estimation of Maria's peak precipitation return periods may be overestimated given the length of the historical record. However, the lower bound of the risk ratios in Figures 3c and 3d are stable over the range of all maximum precipitation values, including historically observed levels and those far exceeding that of Maria, suggesting that the changes in extreme statistics are robust. Almost half of the stations exhibit large reductions in return period estimates through the record with Maria's peak precipitation estimated to be much more likely in recent years. When stations are aggregated into large and small regions both agglomerations show a halving of Maria's estimated return period during the record.

Puerto Rico exhibits large variability in its hydroclimate at inter and intra-annual timescales as a result of the random passage of tropical systems and other heavy precipitation producing events such as easterly waves, cold fronts, and convective storms. Since 1956, 129 tropical storms have passed within 500 km of the island and together Puerto Rico and Hawaii account for 32% of the observed flows above the 99th percentile of all unit discharges in the United States despite representing less than 5% of all observations (O'Connor & Costa, 2004). Such extreme variability present within the historical record across Puerto Rico has likely made EVA estimation of return periods and risk ratios difficult and may account for both the lack of stations with significant physical covariate-based models and lack of those with likely lower bounds of relative risk above one.

Data limitations and the inherent stochastic nature of rainfall in Puerto Rico have restricted our ability to reach definitive conclusions on the relationships between Maria's precipitation and climate variability and change. Only 19 of 34 stations saw improvement over null models through introduction of physical covariates, but ENSO was not statistically significant as a covariate suggesting that modes of Atlantic variability and long-term trends related to human-induced climate change have more influence here. Nine (of 17) stations in the small region of the island, which was most affected by Maria's precipitation, have likely lower bounds of relative risk above one indicating a significant long-term climate trend influence on the storm's precipitation there. Further studies based on dynamical modeling are needed to confirm this finding.

Acknowledgments

The authors would like to thank the student research assistants Eric Riordan and Claire Leone for their contributions to the introduction and data sections of this paper. The daily rainfall data supporting this article are based on publicly available measurements from the National Centers for Environmental Information (NCEI; ftp://ftp.ncdc.noaa.gov/pub/data/ghcn/daily/). The 6-hourly tropical cyclone track data supporting this article are based on publicly available measurements from the International Best Track Archive for Climate Stewardship (IBTrACS; https://www.ncdc.noaa.gov/ibtracs/). This research was supported by the Research, Scholarship, and Creative Activities Program (RSCAP) at Sonoma State University under project MG18010.

References

Bennett, S., & Mojica, R. (1998). Hurricane Georges preliminary storm report: From the tropical Atlantic to the US Virgin Islands and Puerto Rico. San Juan, Puerto Rico.

Coles, S. (2001). *An introduction to statistical modeling of extreme values. Book*, *Springer Series in Statistics*. London: Springer-Verlag. https://doi.org/10.1007/978-1-4471-3675-0

Colon, T., & Jose, A. (2009). Climatologia de Puerto Rico. La Editorial Universidad de Puerto Rico. San Juan.

Cooley, D., Nychka, D., & Naveau, P. (2007). Bayesian spatial modeling of extreme precipitation return levels. *Journal of the American Statistical Association*, *102*(479), 824–840. https://doi.org/10.1198/016214506000000780

Deser, C., Phillips, A. S., & Alexander, M. A. (2010). Twentieth century tropical sea surface temperature trends revisited. *Geophysical Research Letters*, *37*, L10701. https://doi.org/10.1029/2010GL043321

Elsner, J. B. (2006). Evidence in support of the climate change-Atlantic hurricane hypothesis. *Geophysical Research Letters*, *33*, L16705. https://doi.org/10.1029/2006GL026869

Emanuel, K. (2005). Increasing destructiveness of tropical cyclones over the past 30 years. *Nature*, *436*(7051), 686–688. https://doi.org/10.1038/nature03906

Emanuel, K. (2017). Assessing the present and future probability of Hurricane Harvey's rainfall. *Proceedings of the National Academy of Sciences*, *114*(48), 12,681–12,684. https://doi.org/10.1073/pnas.1716222114

Enfield, D. B., Mestas-Nunez, A. M., & Trimble, P. J. (2001). The Atlantic Multidecadal Oscillation and its relation to rainfall and river flows in the continental U.S. *Geophysical Research Letters*, *28*(10), 2077–2080. https://doi.org/10.1029/2000GL012745

Furrer, E. M., Katz, R. W., Walter, M. D., & Furrer, R. (2010). Statistical modeling of hot spells and heat waves. *Climate Research*, *43*(3), 191–205. https://doi.org/10.3354/cr00924

Granger, C. W. J. (1969). Investigating causal relations by econometric models and cross-spectral methods. *Econometrica*, *37*(3), 424. https://doi.org/10.2307/1912791

Hansen, J., Ruedy, R., Sato, M., & Lo, K. (2010). Global surface temperature change. *Reviews of Geophysics*, *48*, RG4004. https://doi.org/10.1029/2010RG000345

Hebert, P. (1976). Atlantic hurricane season of 1975. *Monthly Weather Review*, *104*(4), 453–465. https://doi.org/10.1175/1520-0493(1976)104<0453:AHSO>2.0.CO;2

Hebert, P. (1980). Atlantic hurricane season of 1979. *Monthly Weather Review*, *108*(7), 973–990. https://doi.org/10.1175/1520-0493(1980)108<0973:AHSO>2.0.CO;2

Hernández Ayala, J. J., Keellings, D., Waylen, P. R., & Matyas, C. J. (2017). Extreme floods and their relationship with tropical cyclones in Puerto Rico. *Hydrological Sciences Journal*, *62*(13), 2103–2119. https://doi.org/10.1080/02626667.2017.1368521

Hernández Ayala, J. J., & Matyas, C. J. (2016). Tropical cyclone rainfall over Puerto Rico and its relations to environmental and storm-specific factors. *International Journal of Climatology*, *36*(5), 2223–2237. https://doi.org/10.1002/joc.4490

Hernández Ayala, J. J., & Matyas, C. J. (2018). Spatial distribution of tropical cyclone rainfall and its contribution to the climatology of Puerto Rico. *Physical Geography*, *39*(1), 1–20. https://doi.org/10.1080/02723646.2017.1354416

Hurrell, J. W. (1995). Decadal trends in the North Atlantic Oscillation: Regional temperatures and precipitation. *Science*, *269*(5224), 676–679. https://doi.org/10.1126/science.269.5224.676

Katz, R. W., Parlange, M. B., & Naveau, P. (2002). Statistics of extremes in hydrology. *Advances in Water Resources*, *25*(8-12), 1287–1304. https://doi.org/10.1016/S0309-1708(02)00056-8

Keellings, D., & Waylen, P. (2014). Investigating teleconnection drivers of bivariate heat waves in Florida using extreme value analysis. *Climate Dynamics*, *44*(11–12), 3383–3391. https://doi.org/10.1007/s00382-014-2345-8

Kendall, M. G. (1955). *Rank correlation methods*. London: Griffin.

Kishore, N., Marqués, D., Mahmud, A., Kiang, M. V., Rodriguez, I., Fuller, A., et al. (2018). Mortality in Puerto Rico after Hurricane Maria. *The New England Journal of Medicine*, *379*(2), 162–170. https://doi.org/10.1056/NEJMsa1803972

Knapp, K. R., Kruk, M. C., Levinson, D. H., Diamond, H. J., & Neumann, C. J. (2010). The International Best Track Archive for Climate Stewardship (IBTrACS) unifying tropical cyclone data. *Bulletin of the American Meteorological Society*, *91*(3), 363–376. https://doi.org/10.1175/2009BAMS2755.1

Mann, M. E., & Emanuel, K. A. (2006). Atlantic hurricane trends linked to climate change. *Eos*, *87*(24), 233. https://doi.org/10.1029/2006EO240001

Meléndez, E., & Hinojosa, J. (2017). Estimates of post-Hurricane Maria exodus from Puerto Rico. Centro Voices.

National Academies of Sciences, Engineering, and Medicine (2016). *Attribution of extreme weather events in the context of climate change*. Washington, DC: The National Academies Press. https://doi.org/10.17226/21852

O'Connor, J. E., & Costa, J. E. (2004). Spatial distribution of the largest rainfall-runoff floods from basins between 2.6 and 26,000 km2in the United States and Puerto Rico. *Water Resources Research*, *40*, W01107. https://doi.org/10.1029/2003WR002247

Pall, P., Wehner, M. F., & Stone, D. (2014). Probabilistic extreme event attribution. In P. Pall (Ed.), *Dynamics and predictability of large-scale, high-impact weather and climate events* (pp. 37–46). Cambridge: Cambridge University Press.

Pasch, R., & Avila, L. (1999). Atlantic hurricane season of 1996. *Monthly Weather Review*, *127*(5), 581–610. https://doi.org/10.1175/1520-0493(1999)127<0581:AHSO>2.0.CO;2

Pasch, R., Avila, L., & Guiney, J. (2001). Atlantic hurricane season of 1998. *Monthly Weather Review*, *129*(12), 3085–3123. https://doi.org/10.1175/1520-0493(2001)129<3085:AHSO>2.0.CO;2

Pasch, R., Penny, A., & Berg, R. (2018). Tropical cyclone report Hurricane Maria (AL152017). Miami, FL.

Patricola, C. M., Saravanan, R., & Chang, P. (2014). The impact of the El Niño-Southern oscillation and Atlantic meridional mode on seasonal Atlantic tropical cyclone activity. *Journal of Climate*, *27*(14), 5311–5328. https://doi.org/10.1175/JCLI-D-13-00687.1

Patricola, C. M., & Wehner, M. F. (2018). Anthropogenic influences on major tropical cyclone events. *Nature*, *563*(7731), 339–346. https://doi.org/10.1038/s41586-018-0673-2

Photiadou, C., Jones, M. R., Keellings, D., & Dewes, C. F. (2014). Modeling European hot spells using extreme value analysis. *Climate Research*, *58*(3), 193–207. https://doi.org/10.3354/cr01191

Pielke, R. A., Rubiera, J., Landsea, C., Fernández, M. L., & Klein, R. (2003). Hurricane vulnerability in Latin America and the Caribbean: Normalized damage and loss potentials. *Natural Hazards Review*, *4*(3), 101–114. https://doi.org/10.1061/(ASCE)1527-6988(2003)4:3(101)

Risser, M. D., & Wehner, M. F. (2017). Attributable human-induced changes in the likelihood and magnitude of the observed extreme precipitation during Hurricane Harvey. *Geophysical Research Letters*, *44*, 12,457–12,464. https://doi.org/10.1002/2017GL075888

Santos-Burgoa, C., Sandberg, J., Suárez, E., Goldman-Hawes, A., Zeger, S., Garcia-Meza, A., et al. (2018). Differential and persistent risk of excess mortality from Hurricane Maria in Puerto Rico: a time-series analysis. *Lancet Planet Health*, *2*(11), e478–e488. https://doi.org/10.1016/S2542-5196(18)30209-2

Van Oldenborgh, G. J., Van Der Wiel, K., Sebastian, A., Singh, R., Arrighi, J., Otto, F., et al. (2017). Attribution of extreme rainfall from Hurricane Harvey, August 2017. *Environmental Research Letters*, *12*(12). https://doi.org/10.1088/1748-9326/aa9ef2

Webster, P. J., Holland, G. J., Curry, J. A., & Chang, H.-R. (2005). Changes in tropical cyclone number, duration, and intensity in a warming environment. *Science*, *309*(5742), 1844–1846. https://doi.org/10.1126/science.1116448